Effect of Magnetic Field Annealing on Microstructure and Magnetic Properties of FeCuNbSiB Nanocrystalline Magnetic Core with High Inductance

Xingdu Fan, Fangliang Zhu, Qianqian Wang, Mufeng Jiang[1], Baolong Shen*

School of Materials Science and Engineering, Southeast University, Nanjing 211189, China
[1]Londerful New Material Technology Corp., Nantong 226233, China

*Correspondence to:
Shen BL,
Tel: +86-25-52091077
Fax: +86-25-52091077
E-mail: blshen@seu.edu.cn

Transverse magnetic field annealing (TFA) was carried out on $Fe_{73.5}Cu_1Nb_3Si_{15.5}B_7$ nanocrystalline magnetic core with the aim at decreasing coercivity (H_c) while keeping high inductance (L_s). The magnetic field generated by direct current (DC) was applied on the magnetic core during different selected annealing stages and it was proved that the nanocrystalline magnetic core achieved lowest H_c when applying transverse field during the whole annealing process (TFA1). Although the microstructure and crystallization degree of the nanocrystalline magnetic core exhibited no obvious difference after TFA1 compared to no field annealing, the TFA1 sample showed a more uniform nanostructure with a smaller mean square deviation of grain size distribution. H_c of the nanocrystalline magnetic core annealed under TFA1 decreased along with the increasing magnetic field. As a result, the certain size nanocrystalline magnetic core with low H_c of 0.6 A/m, low core loss (W at 20 kHz) of 1.6 W/kg under flux density of 0.2 T and high L_s of 13.8 μH were obtained after TFA1 with the DC intensity of 140 A. The combination of high L_s with excellent magnetic properties promised this nanocrystalline alloy an outstanding economical application in high frequency transformers.

Key Words: Nanocrystalline alloy, Transverse magnetic field annealing, Induced magnetic anisotropy, Magnetic property, Inductance

INTRODUCTION

Since the nanocrystalline $Fe_{73.5}Si_{13.5}B_9Nb_3Cu_1$ alloy was first found by Yoshizawa in 1988, nanocrystalline soft magnetic alloys (Makino, 2012; Ohta & Yoshizawa, 2008; Suzuki et al., 1991a, 1991b; Willard et al., 1998) have attracted great attention due to their excellent soft magnetic properties such as high saturation magnetic flux density (B_s), high initial permeability (μ_i), low coercivity (H_c) and low core loss (P). From then on, three typical nanocrystalline alloy systems have been developed under the trade name of Finemet (Hitachi Matels Ltd., Japan) (Yoshizawa et al., 1988), Nanoperm (MH&W International Corp., USA) (Suzuki et al., 1991a, 1991b) and Hitperm (Carnegie Mellon University, USA)

(Willard et al., 1998). Among these alloys, Nanoperm exhibits high B_s of 1.5~1.7 T but contains expensive and easily oxidized elements (e.g. Zr or Hf). Hitperm possesses high Curie temperature but the H_c is up to 200 A/m and the large amount of additive element Co increases material cost. Compared to the above alloys, Finemet exhibits high μ_i of 100,000, low H_c of 0.53 A/m, as well as convenient production process, thus has been widely applied in electronic components such as transformers, inductors, sensors, filters etc.

The soft magnetic properties of nanocrystalline alloys result from the uniform nanocrystal structure which effectively reduces the magneto-crystalline anisotropy (Herzer, 1990, 1992, 1997, 2005, 2013). In addition, it has been pointed out that magnetic field annealing can further optimize soft

magnetic properties because the uniaxial anisotropy (K_u) induced by magnetic field has been utilized for tailoring the shape of hysteresis loops (Herzer, 1997, 2005, 2013; Ito et al, 2007; Suzuki & Herzer, 2012). The excellent soft magnetic properties of nanocrystalline alloy, such as low H_c and low core loss (W), contribute to energy conservation and environmental protection. On the other hand, inductance (L_s) is also an important parameter of nanocrystalline magnetic core for electronic components application. With larger L_s, the nanocrystalline magnetic core is more sensitive and effective impedance to the alternating current (AC) interference signal, which is more beneficial to application in signal screening, noise filtering and current stabilizing. However, there are few reports about the influence of magnetic field annealing conditions on magnetic properties of nanocrystalline magnetic core with high inductance. Thus, in this work, we investigated the magnetic properties variation for a certain size magnetic core under no field annealing (NFA) and transverse magnetic field annealing (TFA), respectively, with an essential prerequisite of obtaining or keeping high inductance. The relationship between microstructure and magnetic properties under TFA and NFA were also investigated.

MATERIALS AND METHODS

Amorphous ribbons with nominal composition of $Fe_{73.5}Cu_1Nb_3Si_{15.5}B_7$ were prepared by single roller melt spinning. The width and thickness were 10 mm and 20 μm, respectively. Thermal stability was evaluated by differential scanning calorimeter (DSC) under a flowing highly purified argon atmosphere with a heating rate of 0.67℃/s. Melt-spun ribbons were coiled into toroidal core with 20 mm outer diameter and 14 mm inner diameter. Toroidal core samples were annealed under vacuum to develop nanocrystalline structure by transverse magnetic field furnace and the magnetic field was adjusted by current intensity. The core samples were placed in furnace chamber to ensure magnetic field direction parallel to the width of ribbon. Microstructure of annealed samples was identified by X-ray diffraction (XRD) with Cu Kα radiation and transmission electron microscopy (TEM). Grain size was measured by Nano Measurer software (Fudan University, China) for statistical analysis. L_s was measured at a high frequency of 100 kHz and voltage 0.3 V by inductance-capacitance-resistance digital bridge. B_s was measured by a vibrating sample magnetometer under a maximum applied field of 800 kA/m. H_c and maximum permeability (μ_m) were measured by DC B-H loop tracer under a maximum applied field of 800 A/m. Core loss was measured using AC B-H analyzer. The value of inductance and magnetic properties were calculated by averaging three samples annealed in the same condition.

The industrial annealing process for nanocrystalline magnetic core included five stages: I) heat the furnace from room temperature to 330℃; II) keep the furnace temperature at 330℃ for 60 min, then heat the furnace to 480℃; III) keep the furnace temperature at 480℃ for 60 min, then heat the furnace to annealing temperature (T_a); IV) keep the furnace temperature at selected T_a for 60 min; V) cool down to room temperature with a cooling rate about 0.167℃/s. In this study, we developed the TFA process based on the industrial annealing technology by adding transverse field through different annealing stages. Four TFA conditions were carried out, named TFA1, TFA2, TFA3 and TFA4, respectively. TFA1: applying transverse field through annealing stages II, III, IV and V; TFA2: applying transverse field through annealing stages III, IV and V; TFA3: applying transverse field through annealing stages IV and V; TFA4: applying transverse field only through annealing stage V.

RESULTS AND DISCUSSION

In order to investigate the crystallization behavior, isothermal crystallization annealing was performed on $Fe_{73.5}Cu_1Nb_3Si_{15.5}B_7$ amorphous ribbon samples at different temperature. Fig. 1 shows XRD patterns of ribbon samples annealed for 10 min at 480℃, 550℃, 710℃, which are the temperatures lower than the first crystallization temperature T_{x1}, between T_{x1} and the first crystallization peak temperature T_{p1}, just higher than the second crystallization temperature T_{x2}, respectively, as shown on the DSC curve in the insert. The XRD pattern of as-quenched ribbon is also shown for comparison. It is seen from the XRD patterns that the α-Fe(Si) nanocrystals precipitated in the amorphous matrix after annealed at 480℃, but the grain size is too tiny and the volume fraction is too small that only one diffraction peak is detected, which suggests the grain just start to nucleate from
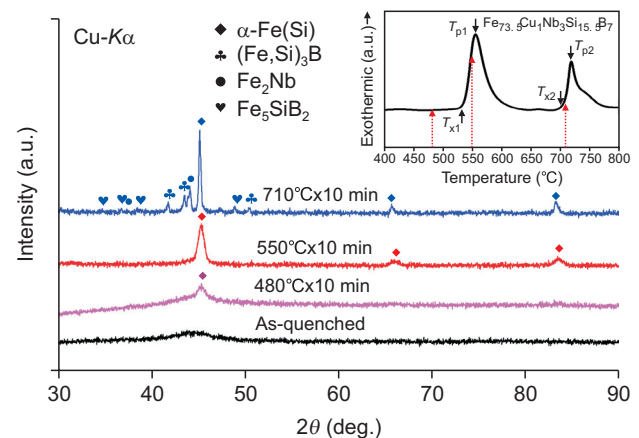
Fig. 1. The X-ray diffraction patterns of ribbon samples annealed for 10 min at 480℃, 550℃, and 710℃ with as-quenched ribbon was showed for comparison. The insert is differential scanning calorimeter curve of $Fe_{73.5}Cu_1Nb_3Si_{15.5}B_7$ melt-spun ribbons. a.u., arbitrary unit; deg., degree.

the amorphous matrix. Three characteristic diffraction peaks of α-Fe(Si) can be identified clearly after annealed at 550℃ which is extremely close to T_{x1}. In contrast, after annealed at 710℃ for 10 min, several Fe-B, Fe-Nb compounds, such as $(Fe,Si)_3B$, Fe_2Nb and Fe_5SiB_2, precipitated and deteriorated soft magnetic property. So it is confirmed that T_{x1} corresponds to the precipitation temperature of single α-Fe(Si) soft magnetic phase and T_{x2} is the crystallization temperature of $(Fe,Si)_3B$, Fe_2Nb and Fe_5SiB_2. The difference between T_{x1} and T_{x2} is 170℃, reflecting the alloy exhibits a preferable thermal stability, which is advantageous for developing nanocrystalline alloys, as it is reported that a wide crystallization temperature difference is beneficial for the precipitation of nanocrystals
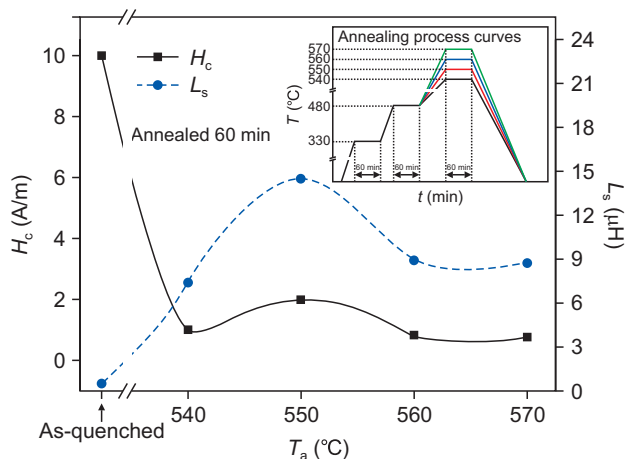

Fig. 2. The dependence of inductance (L_s) and coercivity (H_c) on annealing temperature (T_a) for $Fe_{73.5}Cu_1Nb_3Si_{15.5}B_7$ nanocrystalline magnetic core under isothermal annealing condition compared with no annealing condition sample. The insert is annealing process curves with different T_a (540℃, 550℃, 560℃, and 570℃) in industrial production.

with uniform structure, which can improve the soft magnetic properties (Fan et al., 2013; Makino et al., 1995). Combining the crystallization behavior research results with the industrial manufacturing conditions, the annealing temperature (T_a) in this study are selected as 540℃, 550℃, 560℃, and 570℃, respectively, at which the precipitation of α-Fe(Si) is promoted while the precipitation of hard magnetic phases is inhibited (Hono et al., 1999). The annealing time is fixed as 60 minutes for fully crystallization in order to obtain an ultrafine nanocrystalline structure (Yoshizawa & Yamauchi, 1990).

Fig. 2 shows the dependence of L_s and H_c of nanocrystalline magnetic core samples on T_a under different isothermal annealing conditions. The value of as-quenched alloy is also shown for comparison. The isothermal annealing process, as sketched in the insert in Fig. 2, was designed based on the industrial annealing technology described in the experimental procedures, including five stages: I) heat the furnace from room temperature to 330℃, which is far below T_{x1}; II) keep the furnace temperature at 330℃ for 60 min to ensure heat uniformity in furnace, then heat the furnace to 480℃; III) preserve the furnace temperature at 480℃ for 60 min, which not only keeps inner and outer of the magnetic core samples heat uniformity, but also increases the density of α-Fe(Si) nucleates, then heat the furnace to T_a (540℃, 550℃, 560℃, 570℃, respectively); IV) keep the furnace temperature at each T_a for 60 min, to ensure samples fully crystallization; V) cooling to room temperature. It can be seen that L_s of the core is nearly zero without annealing, but significantly improved after annealing. The value of L_s increases with increasing T_a firstly and reaches its maximum of 14.7 μH at T_a= 550℃, then decreases slightly along with increasing T_a. Meanwhile, the H_c without annealing reaches as high as 10 A/m, but decreases to 1.1 A/m after annealed at 540℃ for 60 min. When T_a rises to
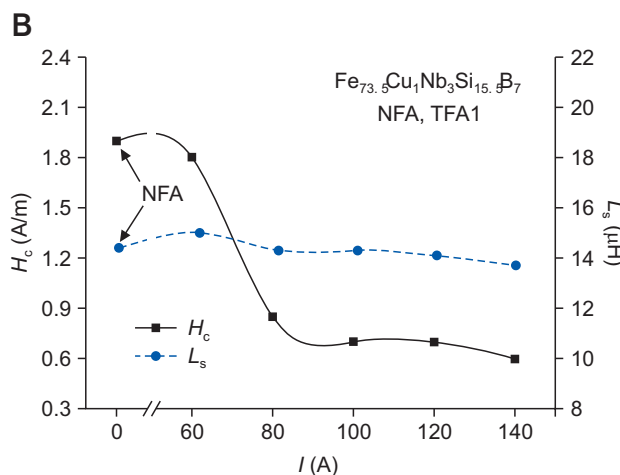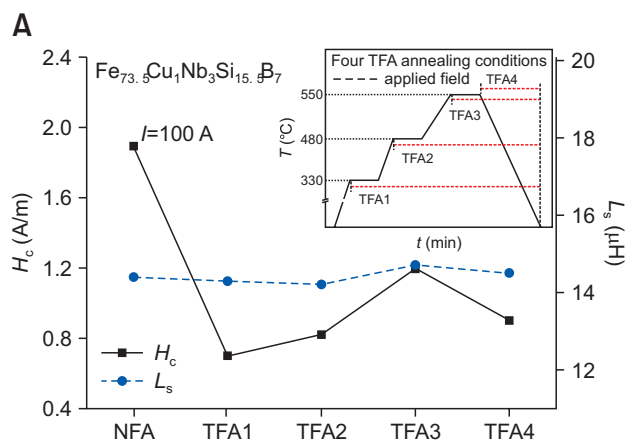
Fig. 3. The dependence of L_s and H_c on (A) four transverse magnetic field annealing (TFA) conditions and (B) TFA1 with different current intensity, together with that of no field annealing (NFA) for $Fe_{73.5}Cu_1Nb_3Si_{15.5}B_7$ nanocrystalline magnetic core. The insert in (A) is four TFA annealing conditions named TFA1, TFA2, TFA3, and TFA4, respectively.
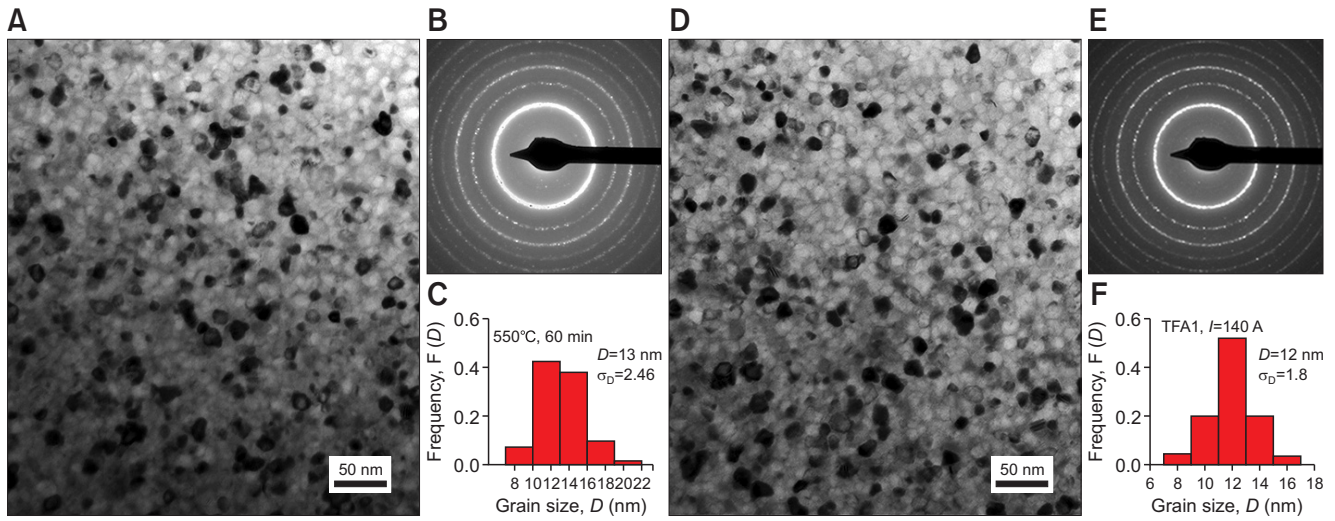
Fig. 4. The bright-field transmission electron microscopy image, selected area electron diffraction pattern and grain size distribution for $Fe_{73.5}Cu_1Nb_3Si_{15.5}B_7$ nanocrystalline magnetic core of (A~C): under no field annealing and (D~F): under transverse magnetic field annealing 1 (TFA 1) with direct current was 140 A.

550℃, H_c increases to 1.9 A/m. As T_a continues increasing to higher than 560℃, H_c decreases to nearly 0.8 A/m. Considering the nanocrystalline magnetic core used in high frequency requires high L_s, the T_a was fixed at 550℃. But the H_c under this annealing condition reached maximum value, so we tried to decrease the coercivity by TFA. Fig. 3A shows the dependence of L_s and H_c of nanocrystalline magnetic core on four TFA conditions, together with that of NFA. The four TFA conditions were carried out by applying transverse magnetic field through different annealing stage, respectively, which named TFA1, TFA2, TFA3, and TFA4 (detail described in the experimental procedures), as shown in the insert in Fig. 3A. The DC intensity in each TFA conditions are all set as 100 A to ensure a constant magnetic field. According to the results, the H_c of sample after NFA is 1.9 A/m. However, when applied transverse magnetic field, H_c decreases remarkably and exhibits the minimum value of 0.7 A/m under TFA1. Meanwhile, L_s almost remains the same value under four TFA conditions. Therefore, the optimum TFA mode is TFA1. To investigate the dependence of L_s and H_c on different magnetic field, we adjusted DC current (I) from 60 A to 140 A under TFA1. The experimental results are shown in Fig. 3B. Similarly, L_s has a slight fluctuation variation, while H_c exhibits sensitive to the current intensity. When I is 60 A, the value of H_c is 1.8 A/m, just a little lower than that of NFA, which suggests the effect of magnetic field is extremely weak under this condition. As I increases to 80 A, H_c decreases rapidly to 0.85 A/m, and then shows a gradually decreasing tendency with increasing current intensity. It is clearly seen that H_c is as low as 0.6 A/m when I increases to 140 A. Hence, we find that at TFA1 condition, the current intensity larger than 80 A is effective for decreasing the H_c. The reason is that

uniaxial anisotropy K_u induced by transvers field annealing dominates over other anisotropies and reduces the coercivity (Herzer, 1997; Suzuki & Herzer, 2012). This is the result we are looking for, that is, not only effectively reducing the H_c, but also maintaining the high L_s.

XRD analyses were performed on $Fe_{73.5}Cu_1Nb_3Si_{15.5}B_7$ nanocrystalline magnetic core samples under NFA condition and TFA1 with different current intensity (results are not shown here). Three characteristic diffraction peaks corresponding to (110), (200), (211) plane, respectively, of α-Fe(Si) phase can be identified for all the NFA and TFA1 samples and there is almost no obvious difference for each sample from the XRD patterns. The average grain size (D) calculated based on (110) plane with Scherrer's equation was 13 nm for all NFA and TFA1 samples. To further understand the microstructure, bright-field TEM and selected area electron diffraction (SAED) analyses were carried out on NFA and TFA1 sample (I=140 A), as shown in Fig. 4. The grain distributions are quite uniform and the volume fractions of nanocrystals are pretty high, which results in identical ultrafine microstructure feature. The diffraction patterns of these two samples from SAED are almost the same. To acquire accurate description of grain size, statistical analysis was carried out by analyzing more than 200 grains for each sample. It is found that the average grain size of NFA and TFA1 (I=140 A) samples are 13 nm and 12 nm, which is consistent with XRD results. However, the grain size of NFA sample mainly range in 10~16 nm, while most nanocrystals of TFA1 (I=140 A) sample are measured as 12 nm. What is more, the mean square deviation (σ) is 1.80 for TFA1 (I=140 A) sample, which is much smaller than that of NFA sample (σ_{NFA}=2.46), reflecting a more uniform nanocrystalline structure. Recently, it was found that

the crystallization reaction rate of Fe-based nanocrystalline (Miglierini et al., 2015; Onodera et al., 2015) is increased by applying extra high magnetic field annealing. It is suggested
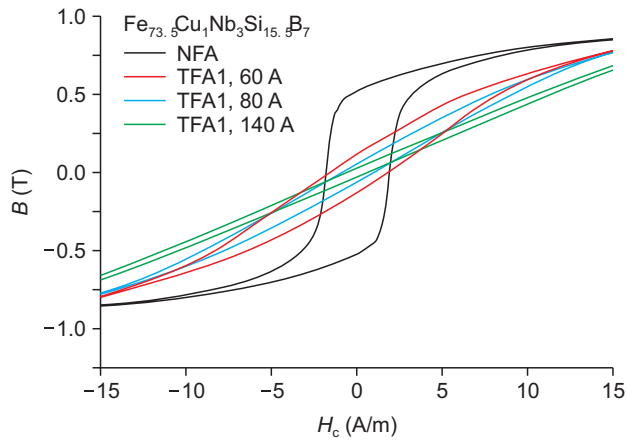
Fig. 5. The characteristics hysteresis loop for $Fe_{73.5}Cu_1Nb_3Si_{15.5}B_7$ nanocrystalline magnetic core under no field annealing (NFA) and transverse magnetic field annealing 1 (TFA1) with direct current were 80 A and 140 A, respectively.

that the nucleation activation energy for primary crystal phase is decreased under field annealing, which results in the increase of nucleation rate and density, whereas the crystallization mechanism is not changed (Fujii et al., 2008; Onodera et al., 2015), so the grain size distribution is more uniform. That is why the mean square deviation of TFA1 (I=140 A) sample is less than that of NFA.

Fig. 5 exemplifies the characteristics hysteresis loops under NFA and TFA1 (I=60 A, 80 A, 140 A) conditions. Obviously, flat loops are obtained after TFA and that the bigger current intensity is, the longer and narrower hysteresis loop becomes. Flat loops means lower magnetic remanence ratio and coercivity and more difficult to be saturated with increasing magnetization, indicating the improvement of anti-DC bias properties of nanocrystalline magnetic core products. Fig. 6 summarizes the dependence of specific magnetic properties (B_s, μ_m and H_c) and grain size (from XRD result) on DC current intensity (I) for $Fe_{73.5}Cu_1Nb_3Si_{15.5}B_7$ nanocrystalline magnetic core samples. The saturation magnetic flux density (B_s) almost stays invariant with current change. It is reported that B_s can be calculated by equation (Ohta & Yoshizawa, 2007)
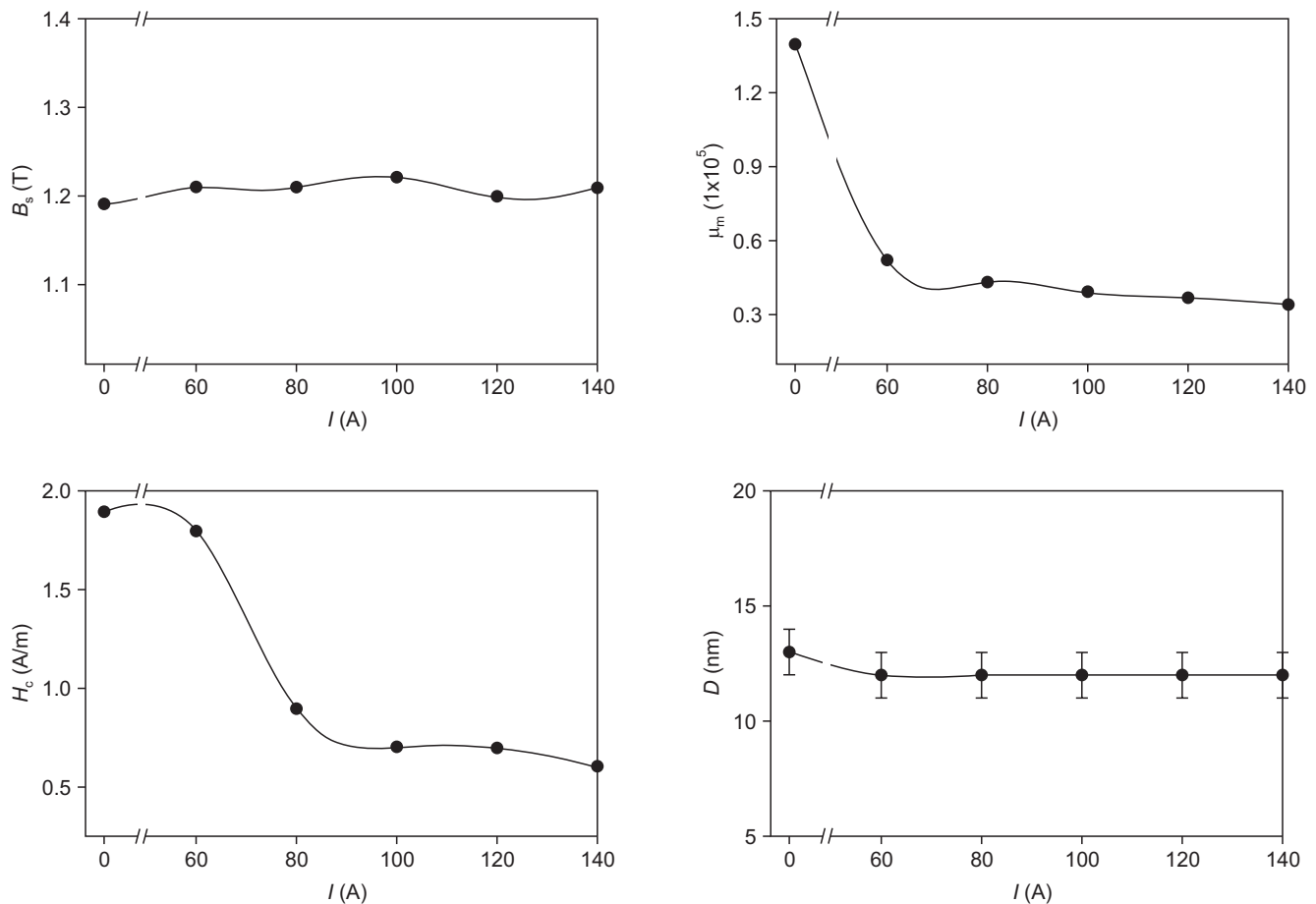
Fig. 6. The dependence of magnetic properties (B_s, μ_m and H_c) and grain size (D) on current intensity for $Fe_{73.5}Cu_1Nb_3Si_{15.5}B_7$ nanocrystalline magnetic core.

$$B_s=B_{sc}V_c/V+B_{sa}V_a/V \qquad (1)$$

where V_c/V and V_a/V stand for the volume fraction of the crystalline phase and the amorphous phase, and B_{sc} and B_{sa} are the saturation magnetic flux densities in the crystalline and amorphous phases, respectively. The constant value of B_s indicates magnetic field annealing does not influence the final volume fraction of crystalline phase for any NFA and TFA1 samples.

Meanwhile, the maximum permeability (μ_m) and H_c shows similar variation tendency with obvious reduction under TFA conditions and reaches the minimum value of 34,000 and 0.6 A/m at I was 140 A, respectively. While μ_m and H_c shows great decrease with increasing current density from 0 A to 80 A, the mean grain size (D_m) has no obvious difference which is about 13 nm for all samples. The result seems to be contrary to the well-known random anisotropy model proposed by Herzer in 1997, 2005, 2013, which suggests that when crystal size is smaller than exchange correlation length ($D<<L_{ex}$), the magneto-crystalline anisotropy $<K_1>$ is essentially reduced by exchange interaction. The overall average anisotropy $<K>$ is approximated by $<K_1>$ and scales down as

$$<K>=<K_1>=|K_1|\cdot x^2 \, (D/L_0)^6 \qquad (2)$$

where x denotes the crystalline volume fraction, L_0 denotes natural ferromagnetic exchange length and $L_0\approx20\sim40$ nm for Fe-based alloys. Since H_c is proportional to $<K>$ and permeability μ is proportional to $<K>^{-1}$, hence $H_c\propto D^6$ while $\mu\propto D^{-6}$. The fact is that the basic anisotropy $<K>$ is attributed to the magneto-crystalline anisotropy K_1, magnetic field induced anisotropies K_u and magneto-elastic anisotropy K_σ. $<K>$ is mainly determined by K_1 under NFA, and equation (2) is valid only under this condition. However, when transverse magnetic field is applied, uniaxial anisotropy K_u, induced with axis parallel to the direction of magnetic field, dominates over other anisotropies and wide transverse slab domains are formed, which largely reduce the H_c and μm (Flohrer & Herzer, 2010; Herzer, 2013; Suzuki & Herzer, 2012). Herzer also has proved that the major contribution to H_c under magnetic field annealing arises from spatial fluctuations of the anisotropy only and the simpler domain configuration (Herzer, 1995). Furthermore, there is a slightly reduction of H_c and μ_m when the current intensity increases from 80 A to 140 A, corresponding to the variation of the flat loop as shown in Fig. 6, which indicates that the Hc and μm are closing to the limit value with the increasing magnetic field under TFA1 condition.

Core loss is extremely important for nanocrystalline magnetic core applied for high frequency electronic components. Fig. 7 shows the dependence of core loss (P) on frequency (f) at 0.2 T for $Fe_{73.5}Cu_1Nb_3Si_{15.5}B_7$ nanocrystalline magnetic core. P increases gradually with increasing f. The increasing rate is small when $f \leq 20$ kHz but accelerate rapidly after that. However, samples under TFA1 condition show obviously slower increasing tendency and the stronger of current intensity is, the slower tendency is. The core loss for TFA1 (I=140 A) sample at 20 kHz is 1.6 W/kg, which is significantly less than that of commercial Finemet alloy of 2.1 W/kg (Yoshizawa et al., 1988). The advantage of low core loss at high frequencies such as 80 kHz and 100 kHz compared to those of NFA magnetic core is extremely obvious. Therefore, the combination of high inductance, low core loss, as well as excellent soft magnetic properties promises application of this nanocrystalline magnetic alloy wide application prospect for high frequency transformers of switched power supplies and interface transformers in telecommunication network.

CONCLUSIONS

Magnetic properties of $Fe_{73.5}Cu_1Nb_3Si_{15.5}B_7$ nanocrystalline magnetic core under NFA and TFA conditions aiming at decreasing the coercivity (H_c) while keeping the high inductance (L_s) were investigated. The main results are summarized as follows: 1. $Fe_{73.5}Cu_1Nb_3Si_{15.5}B_7$ nanocrystalline magnetic core annealed with transverse magnetic field applied during the whole annealing process with annealing temperature 550℃ (TFA1) exhibits the lowest H_c while keeping high L_s compared other annealing conditions. H_c also shows remarkable decrease with increasing DC intensity under TFA1 condition while L_s keeps almost the constant value. 2. The average grain size and crystallization degree of the nanocrystalline magnetic core under NFA and TFA1 conditions exhibit no obvious difference, but the latter shows a more uniform grain size distribution. 3. Uniaxial anisotropy K_u, induced by transverse magnetic field, flattens the hysteresis
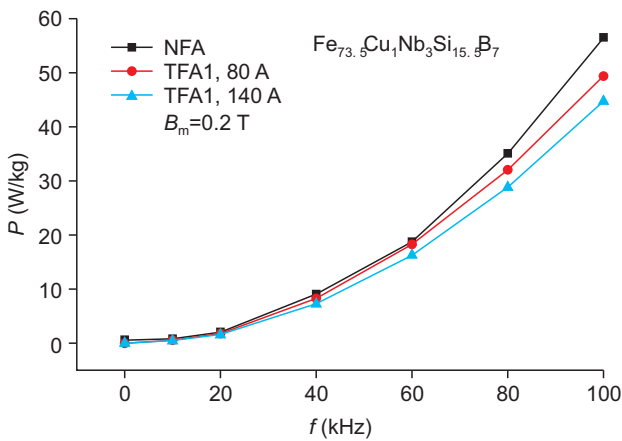
Fig. 7. The dependence of core loss (P) on frequency (f) at 0.2 T for $Fe_{73.5}Cu_1Nb_3Si_{15.5}B_7$ nanocrystalline magnetic core. NFA, no field annealing; TFA1, transverse magnetic field annealing 1.

loop greatly and lowers the maximum permeability and coercivity by dominating over other anisotropies. 4. The nanocrystalline magnetic core under TFA1 with I=140 A exhibits high inductance of 13.8 µH at 0.3 V at 100 kHz and excellent magnetic properties with low coercivity of 0.6 A/m and low core loss (W at 20 kHz) of 1.6 W/kg under flux density of 0.2 T.

CONFLICT OF INTEREST

No potential conflict of interest relevant to this article was reported.

REFERENCES

Fan X D, Men H, Ma A B, and Shen B L (2013) Soft magnetic properties in Fe84-xB10C6Cux nanocrystalline alloys. *J. Magn. Magn. Mater.* **326**, 22-27.

Flohrer S and Herzer G (2010) Random and uniform anisotropy in soft magnetic nanocrystalline alloys (invited). *J. Magn. Magn. Mater.* **322**, 1511-1514.

Fujii H, Yardley V A, Matsuzaki T, and Tsurekawa S (2008) Nanocrystallization of $Fe_{73.5}Si_{13.5}B_9Nb_3Cu_1$ soft-magnetic alloy from amorphous precursor in a magnetic field. *J. Mater. Sci.* **43**, 3837-3847.

Herzer G (1990) Grain size dependence of coercivity and permeability in nanocrystalline ferromagnets. *IEEE Trans. Magn.* **26**, 1397-1402.

Herzer G (1992) Nanocrystalline soft magnetic materials. *J. Magn. Magn. Mater.* **112**, 258-262.

Herzer G (1995) Soft magnetic nanocrystalline materials. *Scripta Metall. Mater.* **33**, 1741-1756.

Herzer G (1997) Nanocrystalline soft magnetic alloys. In: *Handbook of Magnetic Materials*, ed. Buschow K H, pp. 415-462, (Elsevier Science Pub., Amsterdam).

Herzer G (2005) Anisotropies in soft magnetic nanocrystalline alloys. *J. Magn. Magn. Mater.* **294**, 99-106.

Herzer G (2013) Modern soft magnets: amorphous and nanocrystalline materials. *Acta. Mater.* **67**, 718-734.

Hono K, Ping D H, Ohnuma M, and Onodera H (1999) Cu clustering and Si partitioning in the early crystallization stage of an $Fe_{73.5}Si_{13.5}B_9Nb_3Cu_1$ amorphous alloy. *Acta Mater.* **47**, 997-1006.

Ito N, Michels A, Kohlbrecher J, Garitaonandia J S, Suzuki K, and Cashion J D (2007) Effect of magnetic field annealing on the soft magnetic properties of nanocrystalline materials. *J. Magn. Magn. Mater.* **316**, 458-461.

Makino A (2012) Nanocrystalline soft magnetic Fe-Si-B-P-Cu alloys with high B of 1.8-1.9T contributable to energy saving. *IEEE Trans. Magn.* **48**, 1331-1335.

Makino A, Inoue A, and Masumoto T (1995) Nanocrystalline soft magnetic Fe-M-B (M=Zr, Hf, Nb) alloys produced by crystallization of amorphous phase (overview). *Mater. Trans. JIM* **36**, 924-938.

Miglierini M, Procházka V, Rüffer R, and Zbořil R (2015) In situ crystallization of metallic glasses during magnetic field annealing. *Acta Mater.* **91**, 50-56.

Ohta M and Yoshizawa Y (2007) Magnetic properties of nanocrystalline $Fe_{82.65}Cu_{1.35}Si_xB_{16-x}$ alloys (x=0-7). *Appl. Phys. Lett.* **91**, 062517.

Ohta M and Yoshizawa Y (2008) Magnetic properties of high-B_s Fe-Cu-Si-B nanocrystalline soft magnetic alloys. *J. Magn. Magn. Mater.* **320**, e750-e753.

Onodera R, Kimura S, Watanabe K, Yokoyama Y, Makino A, and Koyama K (2015) Nucleation control for fine nano crystallization of Fe-based amorphous alloy by high-magnetic-field annealing. *J. Alloy. Compd.* **637**, 213-218.

Suzuki K and Herzer G (2012) Magnetic-field-induced anisotropies and exchange softening in Fe-rich nanocrystalline soft magnetic alloys. *Scripta Mater.* **67**, 548-553.

Suzuki K, Makino A, Inoue A, and Masumoto T (1991b) Soft magnetic properties of nanocrystalline bcc Fe-Zr-B and Fe-M-B-Cu (M=transition metal) alloys with high saturation magnetization (invited). *J. Appl. Phys.* **70**, 6232-6237.

Suzuki K, Makino A, Kataoka N, Inoue A, and Masumoto T (1991a) High saturation magnetization and soft magnetic properties of bcc Fe-Zr-B and Fe-Zr-B-M (M=transition metal) alloys with nanoscale grain size. *Mater. Trans. JIM* **32**, 93-102.

Willard M A, Laughlin D E, and McHenry M E (1998) Structure and magnetic properties of $(Fe_{0.5}Co_{0.5})_{88}Zr_7B_4Cu_1$ nanocrystalline alloys. *J. Appl. Phys.* **84**, 6773-6777.

Yoshizawa Y, Oguma S, and Yamauchi K (1988) New Fe-based soft magnetic alloys composed of ultrafine grain structure. *J. Appl. Phys.* **64**, 6044-6046.

Yoshizawa Y and Yamauchi K (1990) Fe-based soft magnetic alloys composed of ultrafine grain structure. *Mater Trans. JIM* **31**, 307-314.